Determination of optimal plaster thickness for moisture buffering of indoor air

Dr Daniel Maskell[1], Dr Andrew Thomson[1], Prof Pete Walker[1] and Manfred Lemke[2]

[1]BRE Centre for innovative Construction Materials,
Department of Architecture and Civil Engineering,
University of Bath,
Bath,
United Kingdom

[2]Claytec,
Viersen,
Germany

Corresponding Author: Dr Daniel Maskell, D.Maskell@bath.ac.uk

Keywords

Clay, Moisture Buffering Value, Penetration depth, Hygrothermal properties, Building materials,

Abstract

The relative humidity of indoor air influences the health and wellbeing of building occupants and the integrity of the building fabric. One potential solution for regulating relative humidity is provided by the plaster used for finishing internal spaces if it has the ability to passively buffer moisture through adsorption and desorption of vapour. During the adsorption and desorption, the water vapour will only penetrate to a certain depth of the plaster. Therefore, it is important to know the minimum thickness of plaster required for the maximum buffering effect. Uniquely, this paper presents a method for determining the optimal thickness from experimental measurements on specimens of varying thickness. In this paper it is demonstrated through a novel method, that there is a thickness of material beyond which there is no increase in moisture buffering capacity. Below the optimal thickness moisture sorption increases linearly as a product of the density and specific moisture capacity. Significantly, existing numerical methods were found to overestimate the performance when compared to empirical measurements. The expected impact of this work is the

increased knowledge of surrounding material performance and use, that will ultimately improve the indoor environment quality of buildings and occupant health.

1 Introduction

Hygroscopic materials help to passively regulate the humidity of the indoor environment. The use of these materials can therefore have beneficial impacts on internal comfort levels and operational energy use [Osanyintola and Simpson 2006], [Woloszyn et al 2009], as well as improvements to the health and wellbeing of occupants [Crump et al., 2009]. The Relative Humidity (RH) of an indoor environment is closely related to measures of the Indoor Air Quality and in particular, maintaining RH levels between 40-60% [Rode et al., 2005] is beneficial to the health of building occupants, reducing risks from agents such as bacteria, viruses, chemical reactions, allergies and respiratory infections.

When RH changes, the difference in the vapour partial pressure results in hygroscopic materials adsorbing or desorbing moisture in order to reach equilibrium. This responsive capacity is commonly referred to as moisture buffering and can vary greatly between different building materials [Rode et al., 2005], [Padfield 1998]. The effectiveness of a material is related to the surface area available for vapour exchange, porosity and other hygroscopical properties of the material.

While a moisture buffering capacity can be observed for a variety of materials, the unique physiochemical properties of clay make it an excellent material for this purpose [McGregor et al., 2016]. Clay is used as a construction material in a variety of applications that include structural rammed earth or masonry blocks and as a finishing plaster. Consequently, the range in thickness of earth construction exposed to an indoor environment varies from 3mm of clay plaster, to 400 mm or more for a structural wall. The depth of clay that affects indoor RH levels is dependent on environmental conditions and material properties. A material's rate of moisture

sorption and storage capacity will ideally be balanced with the rate at which airborne moisture is generated during daily peaks of activity.

Padfield [1998] demonstrated a higher moisture buffering potential for clay based materials when compared to many other conventional materials. This is shown in Figure 1 where clay based plaster specimens display a much greater mass change compared to lime or gypsum when exposed to the same cyclic changes in relative humidity over time.

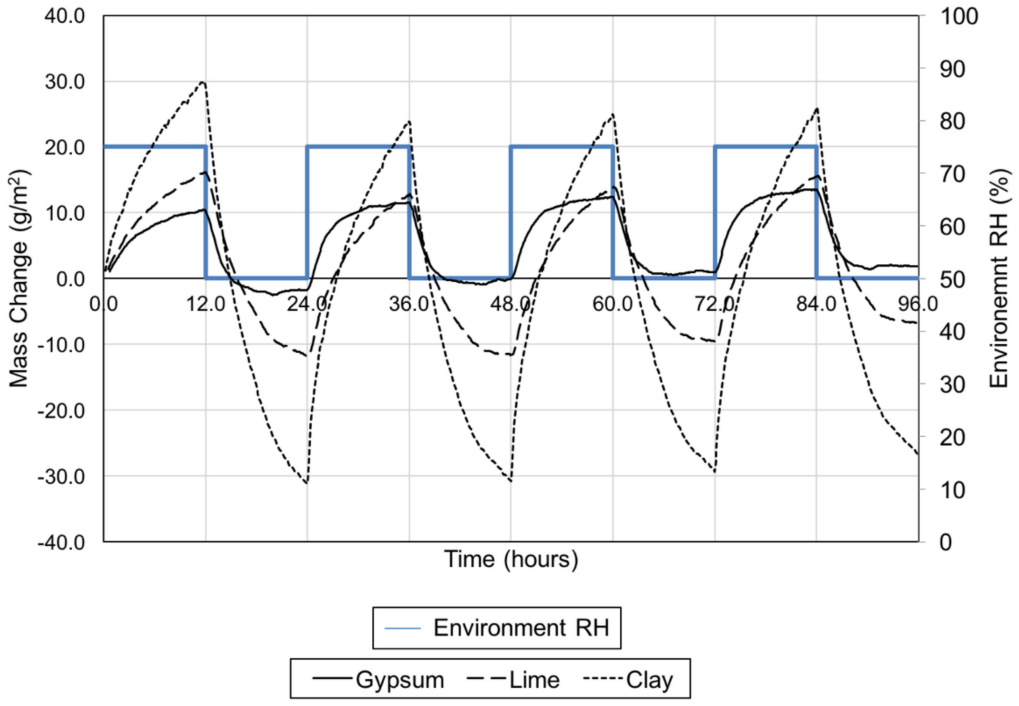

Figure 1 Mass change of plasters when exposed to changing relative humidity at 23 °C

With a view to exploiting the potential of moisture buffering capacity in buildings, plasters are being given increased consideration due to their direct exposure to the indoor environment and large surface area (McGregor et al., 2016, Maskell et al., 2015, Thomson et al., 2015). In addition to plaster materials, there has been a recent increased focus on research into the moisture buffering properties of materials that would not typically be exposed directly to the indoor environment. This includes

hygrothermal insulation materials such as hemp lime [Collet et al., 2013], [Latif et al., 2015] and structural materials such as earth masonry [McGregor et al., 2014a], [Ashour et al., 2015]. However, whilst these materials have an inherent capacity to buffer RH, they are typically covered by a plaster coating and therefore the properties of the plaster may be considered most significant for buffering daily peaks in RH.

Within a fluctuating RH environment typical of indoor conditions, the sorption kinetics will mean that moisture can only penetrate to a certain depth during adsorption before desorption begins. Svennberg (2006) reviewed the definitions of penetration depth or the concept of an active surface layer (as used by Künzel and Kießl 1990) and while different test methods assume different fluctuations they are commonly based on a cyclic period to represent daily generation of moisture through occupancy.

Svennberg (2006) recognised the limitation of a dynamic test method when the penetration depth of the moisture would be greater than that of the specimen thickness. However, this limitation can be beneficially used to empirically determine the moisture buffering depth of a material as illustrated in Figure 2. Beyond this limit of moisture penetration there is no advantage of additional material on the moisture buffering properties, and so it can be defined as an optimal thickness for moisture buffering. Knowing the optimal penetration depth of a plaster will subsequently aid the multi-criteria specification of materials (Maskell et al., 2017) and the design of spaces for enhanced regulation of the indoor relative humidity.

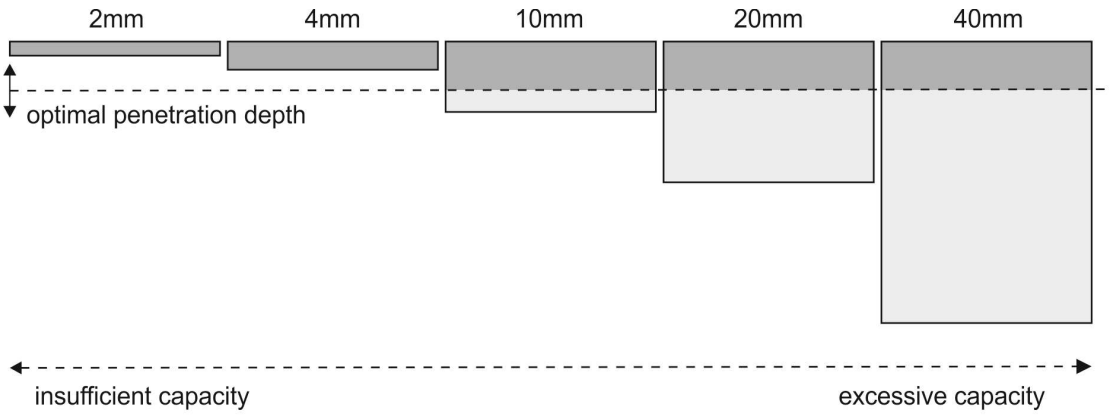

Figure 2 Representation of optimal moisture penetration depth following a period of raised relative humidity

The aim of this paper is to empirically determine the depth of clay plaster that contributes to buffering the RH of indoor air and to use these results to critically assess published analytical methods. This has been achieved through the completion of a series of moisture buffering tests on varying thicknesses of two different clay plasters, which fall below and above the effective moisture penetration depth. In addition to the optimal penetration depth of these materials being established, the test methodology is readily transferable to other materials. The impact of this study is the ability to specify the minimum thickness of plaster that results in the maximum level of humidity regulation.

2 Theoretical Penetration Depth

Whilst the focus of this research is the experimental investigation of the optimal penetration depth of plasters, there are various methods of calculating a theoretical penetration depth (McGregor et al, 2016), which provides an important context for this paper. Variation of moisture within a specimen exposed to a periodically changing relative humidity environment is discussed by Arfvidsson (1999) and Woods et al. (2013) who comment that there is a difference in approach for short term and long term buffering effects.

The theoretical moisture penetration depth of a sample can be calculated using Kirchhoff potentials that describe moisture transport (Rode et al., 2005). The NORD test methodology (Rode et al., 2005) and Wan et al., (2017) propose a simplified method for an approximation based on a sinusoidal variation of the surface moisture content, u, over an amplitude of Δu_s. Assuming that an exponential decrease in amplitude from the surface to a depth dp, Δu_{dp} is given by Equation 1. The relative humidity variation within the specimen reduces with increasing depth to a constant, representing a stable relative humidity during fluctuating external conditions. The calculated 'penetration depth', is typically determined for a humidity variation that is either 100/e% or 1% of the surface variation (McGregor et al., 2016).

$$\frac{\Delta u_{dp}}{\Delta u_s} = \mathrm{e}^{-dp\sqrt{\frac{\pi}{D_w t_p}}} \qquad [1]$$

where; t_p is the cycle time period (s)

D_w (m^2/s) is the moisture diffusivity and is expressed as:

$$Dw = \frac{\delta_p P_s}{\rho \xi_u} \qquad [2]$$

δ_p is water vapour permeability (kg/(m•s•Pa)),

P_s is the saturation vapour pressure (Pa),

ρ is the dry density of the material (kg/m^3)

ξ_u is the specific moisture capacity (kg/kg) and expressed as:

$$\xi_u = \frac{\partial \mathrm{u}}{\partial \varphi} \qquad [3]$$

u is moisture content (kg/kg),

φ is relative humidity.

The specific moisture capacity and water vapour permeability can be calculated from two separate test methods. The specific moisture capacity is calculated directly from Dynamic Vapour Sorption (DVS), whereas the water vapour permeability is calculated as part of the determination of the vapour diffusion resistance factor, μ;

$$\mu = \frac{\delta_a}{\delta_p} \quad [4]$$

where: δ_a is the vapour permeability of air (kg/(m•s •Pa))

The vapour permeability is calculated from:

$$\delta_p = \mathrm{W} \cdot \mathrm{d} \quad [5]$$

where: d is the test specimen thickness (m).

W is the water vapour permeance (kg/(m^2 •s •Pa)) calculated from:

$$\mathrm{W} = \frac{G}{A \cdot \Delta \mathrm{p}} \quad [6]$$

A is the surface area of the specimen (m^2),

Δp is the vapour pressure difference caused by the different RH (Pa),

G is the vapour flow rate (kg/s) and is determined experimentally.

The theoretical moisture penetration depth from Equation 1 is dependent on the effectiveness of penetration, and the assumption of decrease in amplitude of moisture content variations. The NORD test proposes that the ratio should be taken as 1% and therefore Equation 1 can be rearranged and solved for the penetration depth, $dp_{1\%}$:

$$\mathrm{dp}_{1\%} = 4.61\sqrt{\frac{D_w t_p}{\pi}} \quad [7]$$

However, it is noted in the NORD test protocol that Equation 7 is only valid for a semi-infinite or very thick material so its validity to plasters may be questionable. Woods et al., (2013) provide a model for short term moisture buffering effects by assuming the ratio of the amplitudes is given by *1/e,* which is approximately 36.8% therefore Equation 1 for this assumption of penetration depth ($dp_{1/e}$) becomes;

$$\mathrm{dp}_{1/\mathrm{e}} = \sqrt{\frac{D_w t_p}{\pi}} \qquad [8]$$

The methods for estimation of the penetration depth given by Equations 7 and 8 both rely on measurements of the vapour permeability and the isothermal sorption curve. These indirect measurements introduce potential variability that a direct measurement method could mitigate against. This is because a direct measurement of penetration depth would provide an absolute result for a given cyclic humidity regime. The models given in Equation 7 and 8 are also based on assumed decreases in the amplitude of moisture content at a given depth, which, depending on the method chosen, can lead to a factor of 4.61 difference. Therefore, a direct method of determining penetration depth is not only preferential but can also be used to validate models.

3 Materials and Methods

3.1 Materials

Two commercially available clay plasters were selected for the study (Figure 3). These engineered plasters are representative of base and top coat mixes, conforming to the only European standard for clay plasters: DIN 18947. Clay was chosen due to its pronounced moisture buffering capacity as demonstrated in Figure 1. The use of clay was therefore expected to most clearly demonstrate an optimal moisture buffering depth within the range of practical application thicknesses.

The two test plasters have subtly different physical and chemical properties, which will therefore yield different moisture buffering results. For reference the two standard mixes will be termed ‘Top coat’ and ‘Base coat’. The Top coat plaster is a clay, sand and flax fibre mix and the Base coat plaster is a clay and sand mix. These plasters can be described as Reddish-Brown sandy SILT with a plasticity index typical of low plasticity silts, and the engineering properties given in Table 1, (following EN 1015).

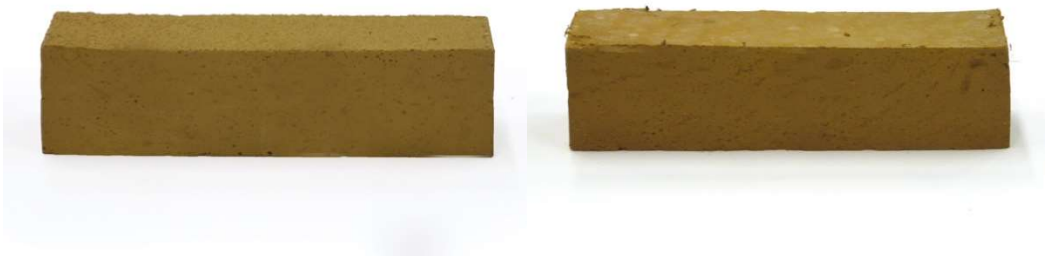

Figure 3 Base coat (left) and Top coat (right) clay plaster specimens

Table 1: Material Characterisation

Properties		Base Coat	Top Coat
Physical Properties			
Liquid Limit	%	14.9	22.1
Plasticity Index	%	1.8	5.7
Linear Shrinkage	%	2.0	4.0
Particle Grading			
Sand	%	69	57
Silt	%	25	37
Clay	%	5	6
Physical Properties			
Bulk Density	kg/m^3	1870	1700
Porosity	%	24.8	30.42
Mechanical Strength			
Compressive Strength	N/mm^2	2.60	2.86
Flexural Strength	N/mm^2	0.97	1.19

3.2 Experimental Methods

The primary aim of this study is the development of an experimental method for the determination of the effective penetration depth for moisture buffering. However, in addition to the measurement of moisture buffering properties, mechanical properties were also determined. All the tests were conducted in triplicate 28 days after casting, with all specimens stored at 23°C and 50% RH prior to testing.

3.3 Physical and mechanical properties

The bulk dry density of the hardened mixes was determined following EN 1015-10 (1999). The flexural and compressive strength was determined in accordance with EN 1015-11 (1999). Specimens were loaded under displacement control at a rate of 0.2 mm/min and 0.5 mm/min for the determination of flexural and compressive strength respectively. The results are presented in Table 1.

3.4 Theoretical penetration depth

The theoretical penetration depth is dependent on two independent measurements from isotherms and vapour diffusion experiments. DVS was used to determine the isotherm in the relative humidity range 0% to 95% at 23 °C. The vapour diffusion properties were determined according to ISO 12572:2001, investigating both wet and dry cup conditions following the climate chamber method.

3.4.1 Dynamic vapour sorption (DVS)

The DVS is a gravimetric technique of measuring mass change due to vapour sorption. The specimen is placed on a micro balance and the surrounding vapour concentration is incrementally changed resulting in a measureable change in mass of the specimen. The sorption isotherm was measured at 23 °C on specimens with a mass of approximately 50mg. The experimental precision in measuring sorption isotherm mass change was ± 0.1 mg; the temperature was maintained to ± 0.1 °C; and, the RH was maintained to ± 1% RH. Although relatively small specimens were used for the measurement, the material is homogenous and therefore considered representative of larger expanses such as plasters (McGregor et al., 2014a).

3.4.2 Vapour diffusion resistance factor

The vapour diffusion resistance factor of the samples was determined according to EN ISO 12572:2001. The specimens were initially conditioned at (23 ± 2) ºC temperature and (50 ± 5)% Relative Humidity to reach a constant mass over 24 hour period. The specimens were placed on plastic cups containing potassium nitrate salt solutions for the ‘wet cup’ test method. The sides of the specimens were sealed with aluminium foil ensuring unidirectional moisture flow. The Relative Humidity inside the dishes was regulated by the salt at 95% while the external conditions were regulated within an environmental chamber at 50% (±3)%. The assembly was weighed and automatically logged at 5 minute intervals until consistent mass loss rate over five days was achieved.

3.5 Moisture buffering test method

There are various methods to characterise the moisture buffering capacity of a material. In Germany one method for clay plaster is described in DIN 18947, but currently no Euro-norm exists. The NORD test (Rode et al., 2005) is widely used, with similar methods used by the Japanese standard (JIS A 1470-1, 2002) and the ISO method (ISO 24353:2008). Roels & Janssen (2006) comment that although there is similarity between the test methods, the differences lead to non-comparable results. Of the three standards, the ISO standard test has ranges of RH and time cycles that are considered representative of indoor occupancy whilst also providing a broad basis for international comparison of data. Therefore it was the method adopted in this study.

The method required specimens to be pre-conditioned at a relative humidity of 63% and a temperature of 23 °C before cyclic climatic variations were started, until there was no change in mass over a 24 hour period. The pre-conditioning and the cyclic tests was undertaken within the same programmable climate chamber. Three chambers that could test two specimens were used simultaneously were used. Preliminary investigation showed that there was no statistical variation in performance based on the testing location in either of the chambers. The cyclic test method for mid-level humidity was adopted. A cycle consisted of a step change between a relative humidity of 75% and 50% every 12 hours whilst the temperature was constant at 23 °C (as indicated by the Environmental RH in Figure 1) . Four of the 24 hour cycles were run whilst the mass of the specimen was logged at 5 minute intervals. A screen was placed around the mass balance to minimize the influence of air movement over the surface of the specimens during testing. An anemometer was used to measure wind speed at the specimen surface and was found to be an average of 0.1 m/s. The vapour surface resistance is assumed to be constant across all tests, however, the impact of the surface resistance is likely to have a greater

effect on the thinner specimens. Fourth cycle moisture adsorption and desorption content values and rates were calculated in accordance with Section 8.3 of ISO 24353:2008.

The three thinnest specimen thicknesses for the moisture buffering tests were prepared in 150 x 150 mm moulds with varying thicknesses of 2, 4, and 10 mm. The moulds were made from acrylic and wrapped in aluminium tape, acting as a permanent formwork. This allowed thin coating thicknesses to be accurately achieved while removing the risk of handling damage of the brittle material. The samples of 20 mm and 40 mm thickness were cast within phenolic plywood moulds, removed following 3 days of initial drying after casting and wrapped in aluminium tape to seal the back and sides. Although this induced slightly different boundary conditions of these specimens, the use of aluminium tape is to ensure vapour exchange occurred only through a single face (with the same surface area) of the material regardless of the thickness, as in Figure 4.

Figure 4. Clay moisture buffering specimens of different thicknesses

4 Results and discussion

4.1 Theoretical penetration depth

The theoretical penetration depth is dependent on two independent measurements from DVS and vapour diffusion experiments.

4.1.1 DVS

The adsorption - desorption isotherm for the top coat and base coat plaster is shown in Figure 5. The curves represent averages of two complete sorption cycles of three samples, with the error bars representing the 95% confidence interval of the mean. Each specimen was run through three sorption cycles with the first cycle omitted from analysis.

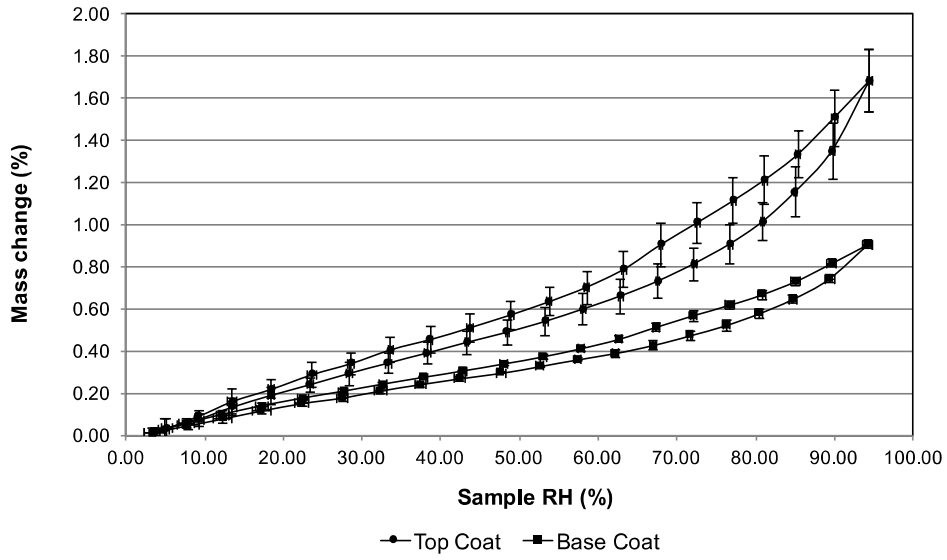

Figure 5 DVS of the two earth plasters

The results indicate the different sorption properties between the top coat and base coat. There is significantly less mass change for changing RH for the samples in Figure 5 when compared to the curves presented by McGregor et al., (2014a). This can be partially attributed to the particle size distributions as seen in Table 1, which show a significant amount of silt and sand size particles. The DVS curves presented by McGregor et al., (2014a) are only those samples of artificial soils with at least 20% clay fraction.

Both sorption curves show 95% confidence intervals based on three samples each having two cycles. The base coat shows insignificant variability in mass at each relative humidity step whereas the top coat plaster shows distinctly greater variability. Although the general trend of sorption can be observed, it does indicate potential variability within the material and questions the assumptions by McGregor et al., (2014a) of homogenous material, and lack of need for repetition.

4.1.2 Vapour diffusion resistance factor

The vapour diffusion resistance factor for the base coat and top coat were measured using the wet cup method using three samples. The vapour resistance factor was measured to be 6.37 and 7.29 for the top and base coat respectively with less than 2% Coefficient of Variation. The vapour resistance factor is less than the plaster samples tested by McGregor et al., (2014a) that are in the range of 8 to 14, but comparable to the Compressed Earth Blocks (CEB) tested. The density of the plasters tested within this paper are similar to the CEB tested by McGregor et al., (2014b), however, there was a variable degree of correlation between density and vapour diffusion resistance factor for different samples.

4.1.3 Calculation of Theoretical Penetration Depth

The theoretical penetration depth based on the isotherms and vapour diffusion resistance for the two coatings can be calculated using Equations 7 and 8. The calculated moisture diffusivity for the top and base coat are 3.176 e-9 m^2/s and 5.649 e-9 m^2/s respectively. Depending on the model of the penetration depth used, this resulted in variable effective moisture buffering depths as presented in table 2.

Table 2: Theoretical effective moisture buffering depth.

Properties	Top Coat mm	Base Coat mm
$dp_{1\%}$	43	57
$dp_{1/e}$	9	12

4.1.4 Discussion of Theoretical Penetration Depth

The theoretical penetration depth is dependent on the experimentally determined moisture capacity from DVS and vapour diffusion properties. As seen in Figure 5, the DVS gives adsorption and desorption curves with a significant hysteresis. While the median value was used for the calculation, the hysteresis will significantly effect the penetration depth and moisture buffering properties. The vapour permeability is identified by 'wet-cup' method in 50%-95% RH range, while cyclic tests are a different RH range, irrespective of whether the ISO method or NORD test method is used. The apparent vapour permeability strongly increases beyond 75% RH, so that the measured permeability is perhaps non-representative of that involved during the cyclic tests.

The theoretical penetration depth assumes the RH boundary conditions change with a sinusoidal variation while the moisture buffering experimentation boundary condition changes with a rectangular variation. This is likely to be an additional source of error. Therefore determining the optimal thickness via moisture buffering experimentation will overcome many of these barriers.

4.2 Optimal penetration depth

The moisture buffering properties of 30 specimens were tested; two clay plaster variants at 5 thicknesses, all in triplicate. The typical mass change profile (from the Base coat samples) is presented in Figure 6. The ISO standard considers only the fourth cycle and calculates the adsorption and desorption mass change per unit of exposed area, and is presented in Table 3, with the Coefficient of Variation presented in parentheses.

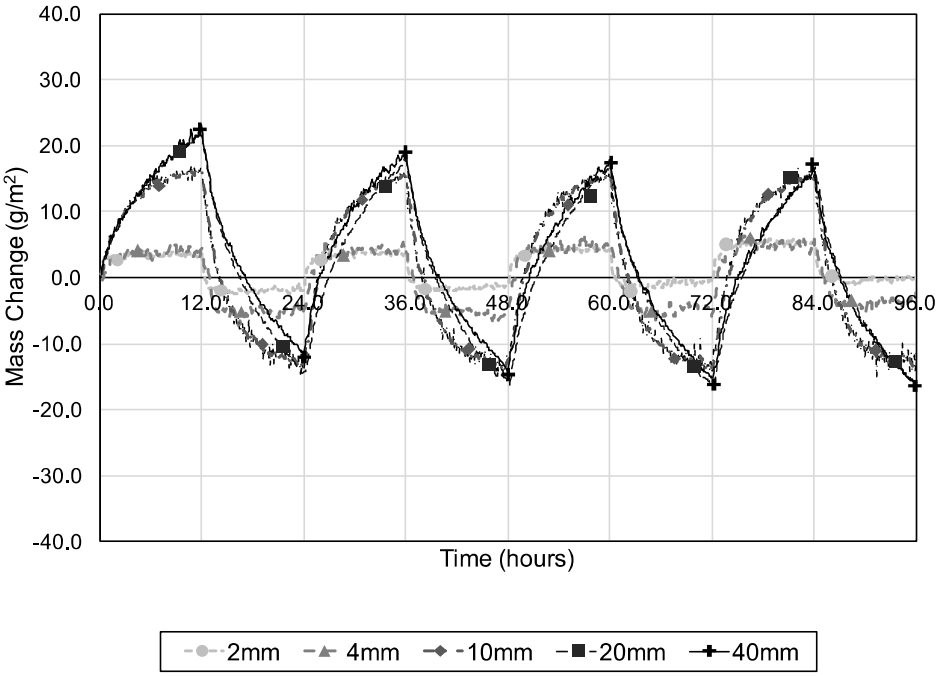

Figure 6 Typical moisture buffering profiles

Table 3 Fourth cycle absorption and desorption properties

Typical Application	Thickness (mm)	Moisture adsorption content for the 4th cycle (g/m^2)	CoV	Moisture desorption content for the 4th cycle (g/m^2)	CoV
Top Coat	2	10.7	(19.1%)	10.0	(17.7%)
	4	27.4	(8.6%)	28.3	(7.3%)
	10	47.3	(3.1%)	49.0	(6.1%)
	20	44.7	(2.6%)	41.9	(4.0%)
	40	45.7	(3.3%)	47.0	(6.4%)
Base Coat	2	9.3	(27.0%)	9.0	(19.2%)
	4	16.8	(4.1%)	17.1	(6.5%)
	10	31.7	(7.9%)	32.7	(4.7%)
	20	34.3	(6.1%)	33.7	(4.5%)
	40	32.0	(10.8%)	33.3	(6.2%)

4.2.1 Effect of moisture thickness on moisture buffering properties

It is clear from Figure 6, and the adsorption and desorption data from Table 3, that the moisture buffering capacity is capped by the thinner plaster specimens as the mass change plateaus early into the humidity cycle. Comparing the profiles of the 40 mm and 20 mm negligible differences are observed, indicating that there is no additional buffering achieved through the extra thickness. The adsorption and desorption of the fourth cycle of the 30 specimens is presented in Figure 7 and 8 respectively, with the error bars representing the 95% confidence interval based on a sample of three specimens.

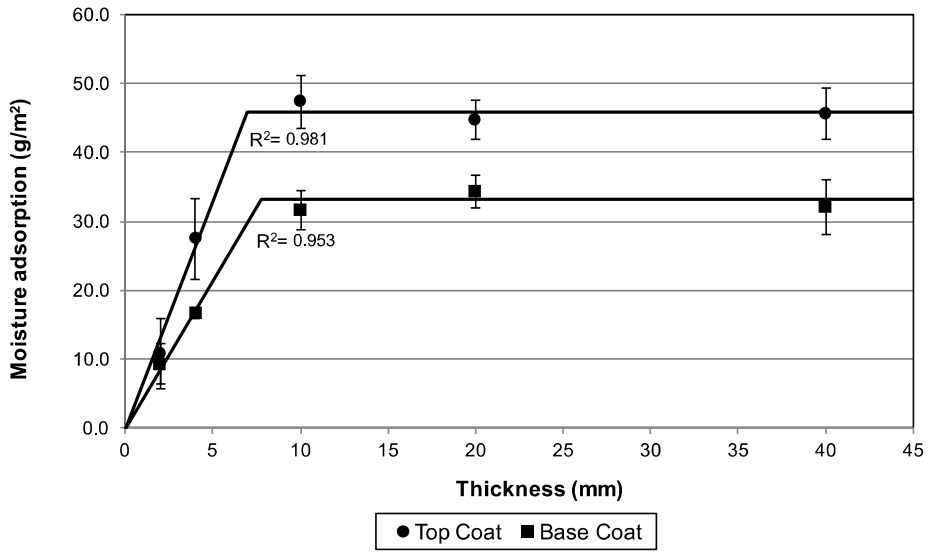

Figure 7 Variation of moisture adsorption with depth

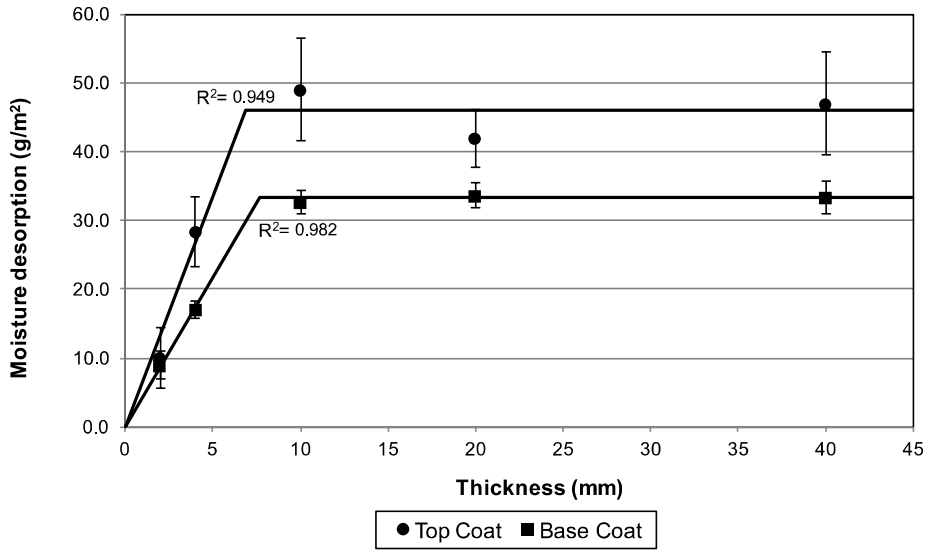

Figure 8 Variation of moisture desorption with depth

4.2.2 Determining the effective penetration depth

From Figures 7 and 8, there is no apparent additional benefit to moisture buffering beyond a 10mm thickness of either type of plaster. Regression is used to predict the moisture adsorption and desorption and can be used to determine an empirical

optimal thickness. The data shows a bi-linear trend that increases linearly up to a optimal thickness, t_{opt}, beyond which point there is no further increase in moisture buffering effect. Where there is an increase in moisture buffering capacity with thickness, the slope of the line can be calculated using a least squares regression, with the assumption that the intercept passes through the origin because zero thickness will result in zero buffering. The plateau can be calculated as the average of the moisture buffering results for the specimens in the 10-40 mm thickness range. This results in equation 9 which describes the experimental findings and is shown graphically in Figure 9:

$$\hat{y} = \begin{cases} \hat{\beta} t, & t < t_{opt} \\ \overline{y_t}, & t \geq t_{opt} \end{cases} \quad [9]$$

where:

$\hat{y}$ is the predicted value of moisture adsorption / desorption

t is the thickness of the material

$\overline{y_t}$ is the mean value of moisture adsorption / desorption for thicknesses greater than t_{opt},

$\hat{\beta}$ is the gradient of a linear regression through the origin for thicknesses less than t_{opt},

Therefore, the optimum thickness, $t_{opt,}$ is the intersection of the two linear regression models described in Equation 9 and is given by Equation 10

$$t_{opt} = \frac{\overline{y_t}}{\hat{\beta}} \quad [10]$$

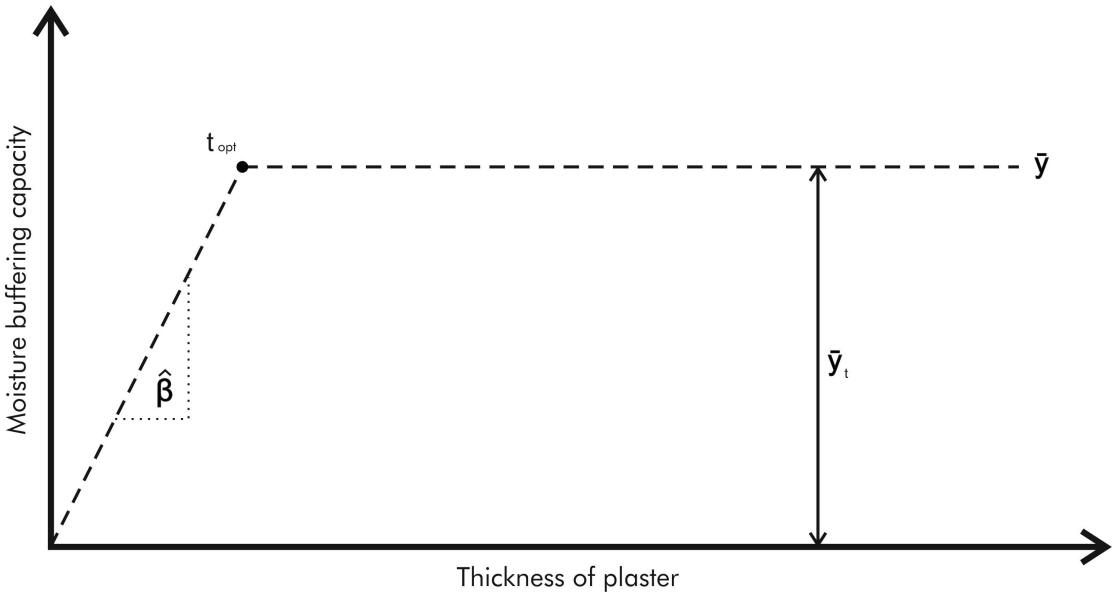

Figure 9 Terminology used to describe bi-linear trend

The model results in a bi-linear trend, based on the linear increase in moisture adsorption calculated by the measurements at 2mm and 4mm and the mean of the values at 10mm and greater. The coefficient of determination, R^2, for the model's prediction of the top and base coat, under adsorption and desorption is at least 0.94, (Figures 7 and 8). This indicates the regression is suitable to model the experimental penetration depth. Theoretically, the moisture buffering effects of a material at fixed experiment settings would gradually reduce and reach an asymptotical limit, and exponential lines could be fitted to the data points in Figures 7 & 8. However, the linear relation is more practical for the real engineering solutions, and would greatly simplify the design to utilise moisture buffering effects of hygroscopic materials in buildings.

For the tested excitation profile, the regression estimates the optimal penetration depth, t_{opt}, for the top and base coat to be 7.1 mm and 7.7 mm during adsorption respectively and 6.9 mm for both coats during desorption. This indicates that the theoretical methods, from Table 2, for the determination of penetration depth overestimate the material required to buffer the tested RH cycle.

While the model has a strong correlation with all measured values, the optimal thickness still represents a single point estimate and the confidence intervals in Figures 7 and 8 indicate the bilinear model could result in different optimum thicknesses if this variability was accounted for. Therefore, an effective confidence interval for the optimum thickness can be considered by accounting for errors in the linear regression within Equation 10. The maximum optimal thickness would be achieved by assuming $\overline{y_t}$ was underestimated and $\hat{\beta}$ was overestimated, and the minimum optimum thickness would be achieved conversely. The amount of error in the optimal thickness value can be approximated by considering an appropriate confidence interval, based on the t-statistic and degrees of freedom (df) of the two linear models separately as represented in Figure 10 and 11. Accounting for 15 degrees of freedom the 95% confidence interval of the model, Equation 10 for the optimum thickness yields a range given by Equations 11 and 12.

$$t_{opt,max} = \frac{\bar{y}_t + df_t \cdot SE_{\bar{y}_t}}{\hat{\beta} - df_t \cdot SE_{\hat{\beta}}} \quad [11]$$

$$t_{opt,min} = \frac{\bar{y}_t - df_t \cdot SE_{\bar{y}_t}}{\hat{\beta} + df_t \cdot SE_{\hat{\beta}}} \quad [12]$$

where:

$t_{opt,max}$ is the maximum optimum thickness

$t_{opt,min}$ is the minimum optimum thickness

df_t is the *t-statistic* based on the degrees of freedom

$SE_{\bar{y}_t}$ is the standard error of the mean of the moisture adsorption / desorption for thicknesses great than t_{opt},

$SE_{\hat{\beta}}$ is the standard error of the gradient of a linear regression through the origin for thicknesses less than t_{opt},

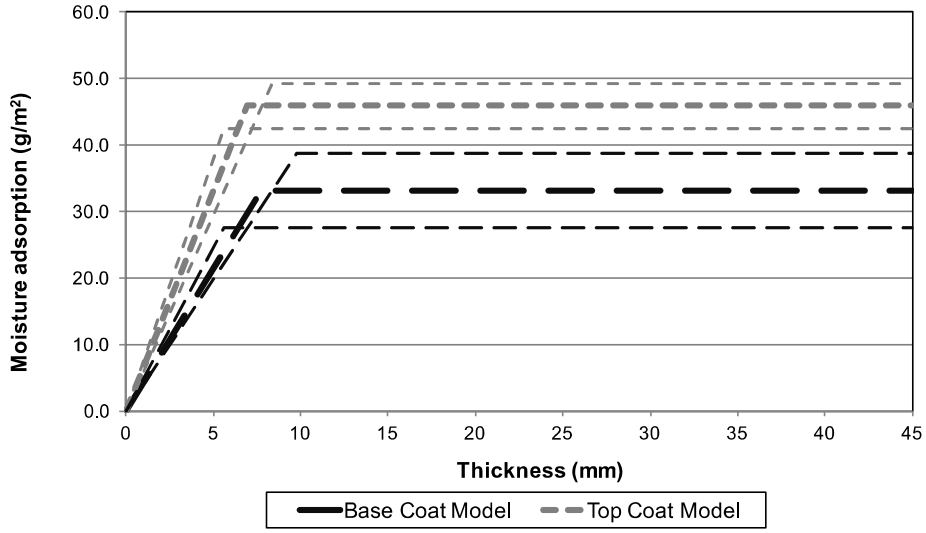

Figure 10 95% Confidence Interval for experimental adsorption penetration depth

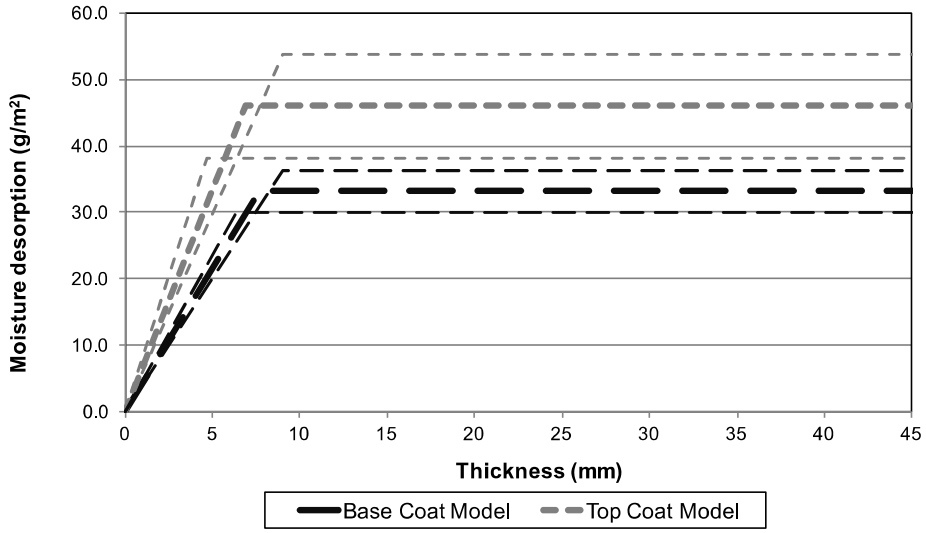

Figure 11 95% Confidence Interval for experimental desorption penetration depth

The range based on 95% confidence interval of the optimum thickness is given for the different coatings under adsorption and desorption in Table 4. The greatest range of optimum thickness was calculated at 4.4 mm for the top coat under desorption,

which is relatively significant compared to the point estimate of t_{opt}. However, the optimal thickness for maximum moisture buffering performance given by $t_{opt,max}$, is still less than that predicated by the theoretical approaches that do not directly measure moisture buffering.

Table 4: Effective 95% confidence interval for optimal thickness for moisture buffering thickness

	$t_{opt,min}$ mm	t_{opt} mm	$t_{opt,max}$ mm
Base Coat - Adsorption	5.6	7.7	9.8
Base Coat - Desorption	6.4	7.7	9.0
Top Coat - Adsorption	5.6	7.0	8.4
Top Coat - Desorption	4.7	6.9	9.1

4.2.3 Discussion

The model developed from equation 10 is based on empirical observations of the clay materials tested. However, the method is likely to be more broadly applicable on the basis that the initial slope and the resulting plateau for different materials and test cycles can be relatively simply characterised, due to the generalised similar behaviour of materials as observed in Figure 1 and Rode et al., (2005). The choice of a daily period for RH variations is not representative of real building environments. Shorter and more complex scenarios could be utilised within the experimental method used within this research and combined with numerical simulation to give fast and straightforward information on the building performance.

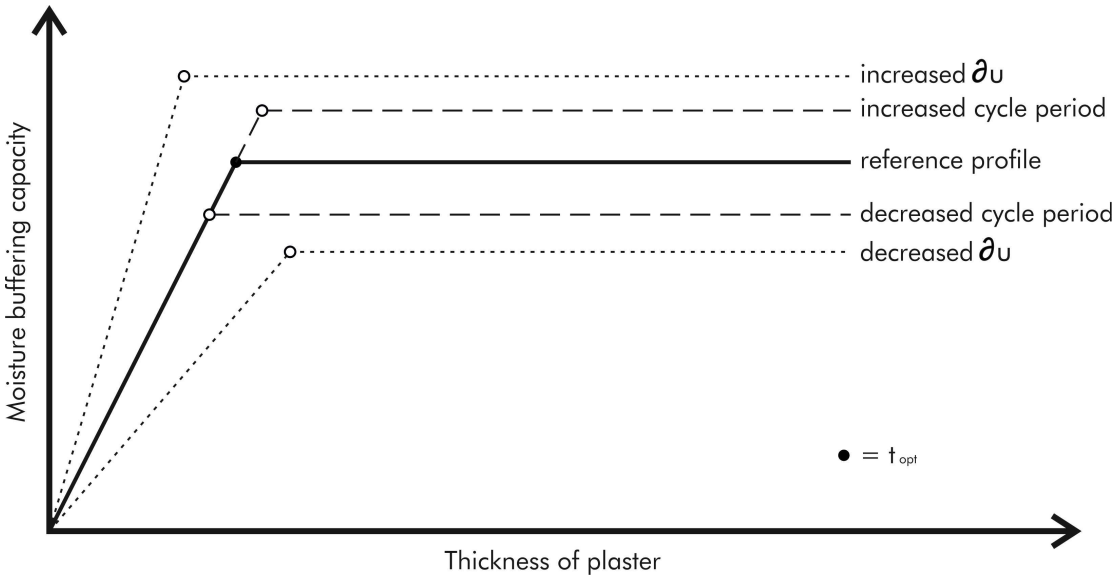

Figure 12 Factors affecting t_{opt} in bi-linear model

Linear regression has been used to calculate the optimal penetration thickness from direct measurement. The model developed in Equation 9 is only dependent on the material's sorption isotherm and the period of the adsorption/desorption cycles. The implications for variance of these two attributes is described in Figure 12. When the thickness of the material is less than the optimal thickness, adsorption and desorption is limited by the capacity of the full thickness of the material, indicating that maximum sorption capacity has been reached. The gradient, $\hat{\beta}$, is therefore logically dependent on the specific moisture capacity, ξ_u, at the specific change in moisture content, or specifically the change in moisture content, between the two environmental conditions tested, such that:

$$\hat{\beta} = \xi\_u \cdot \partial\varphi \cdot \rho$$
$$= \partial u \cdot \rho \qquad [13]$$

Where ∂_u is the change in moisture content of the material for the given RH buffering range and ρ is the dry density of the material. Taking density values from Table 1, change in moisture content for the given change in RH from the DVS (Figure 5) and

the t_{opt} values from Table 4 gives moisture adsorption and desorption values for the two clay materials. Comparing these to those predicted by $\overline{y_t}$ gives a difference of less than 10% and within the 95% confidence interval.

In the literature the plateau is described by the average of the adsorption or desorption capacity, *G* (g/m^2), and this can be normalised with the change in surface relative humidity to give the Moisture Buffering Value (MBV), ((g/(m^2•RH%)) for a given humidity cycle (Rode et al., 2005). Rode et al. (2005) provide a method of calculating this 'idealised' total adsorption/desorption capacity, G_{ideal}, but this is based on a different humidity cycle to that set out in the ISO standard. McGregor et al (2014b) modified this model for a 12h/12h cycle, as used in this study, which resulted in equation 14. This MBV cycle can be expressed with respect to G_{ideal}, as in equation 15:

$$MBV_{ideal} = 0.0061.p_{sat}.b_m.\sqrt{t_p} \quad [14]$$

$$G_{ideal} = 0.0061.p_{sat}.\Delta RH.b_m.\sqrt{t_p} \quad [15]$$

where: $t_{p,}$ is the time period (s)

b_m is the moisture effusivity given by

$$b_m = \sqrt{\frac{\delta_p \cdot \rho_o \cdot \xi_u}{p_s}} \quad [16]$$

where: ρ_o is the density (kg/m^3)

From equation 16, the total idealised adsorption and desorption can be estimated for the top and coat as 69.1g/m^2 and 45.2 g/m^{2}respectively. The measured adsorption values for the top and base coat, from Table 3, are 73.1% and 66.4% of the idealised

values respectively. Rode et al. (2005) acknowledge the non-idealised conditions within an experiment but, nonetheless, using the developed idealised moisture adsorption/desorption value could result in a significant overestimation of capacity. The variation, between the ideal and actual value is attributed by Rode et al., 2005 to either the homogeneity of the material or the thickness in relation to the optimum penetration depth. However, considering that the thickness is significantly thicker than the optimum penetration depth as discussed throughout the paper and the material can be considered homogenous then there are clearly other factors that significantly affect the practical moisture buffering performance. Therefore, the total adsorption/desorption should be measured and used for the determination of the experimental optimum penetration depth.

5 Conclusions

An original method of experimentally determining the optimal moisture buffering depth of plaster materials has been presented. The method has been developed according to the ISO method, but is applicable to other methods. Two types of clay plaster were investigated, with different physical and chemical properties that resulted in different moisture buffering properties. This approach has demonstrated the conceptual approach to experimentally determine the optimal moisture buffering depth of other materials, which would likely vary based on a range of interconnected parameters.

- Moisture sorption isotherms can be sensitive to sampling, particularly when the material is highly adsorbing and in low quantities within a composite, which is common with clay minerals and the resulting plasters;
- There is a optimal thickness of material, beyond which there is no increase in moisture adsorption or desorption capacity for a given excitation profile;

- Below the optimal thickness the moisture sorption capacity was observed to increase linearly with thickness and is based on the density and specific moisture capacity;
- The idealised moisture adsorption values calculated with published non-direct test methods can lead to an overestimation compared with the practical moisture adsorption/desorption capacity measured empirically;
- A bi-linear model can be used to predict an optimal thickness for moisture buffering. This analysis gave lower thickness values than those calculated with existing models. The model has greater practicality in real word applications due to its linearity.

The optimal thickness of a material for moisture buffering can be determined experimentally by two moisture buffering tests. Assuming the optimum thickness is approximately known, a moisture buffering test above and below this thickness will provide sufficient data for the model to predict the thickness. The resulting mass change profiles can be compared to those in Figure 5 to ensure that there are profiles with a distinctive plateau and saw tooth for thicknesses below and above the optimum thickness respectively. Alternatively, a water vapour isotherm will give sufficient experimental results to predict the material's moisture buffering performance below the optimal thickness.

The significance of directly measuring the moisture buffering penetration depth will result in an optimised layer structure for the combined plaster top and base coats resulting in efficient indoor moisture buffering performance. Existing methods for calculating optimal moisture buffering depth appear to be overly conservative for typical building occupancy.

6 Acknowledgements

The research leading to these results has received funding from the European Union's Seventh Framework Programme (FP7/2007-2013) under grant agreement no 609234.

7 References

Arfvidsson, J. (1999). "A New Algorithm to Calculate the Isothermal Moisture Penetration for Periodically Varying Relative Humidity at the Boundary." Nordic Journal of Building Physics 2.

Ashour, T., Korjenic, A., & Korjenic, S. (2015). Equilibrium moisture content of earth bricks biocomposites stabilized with cement and gypsum. *Cement and Concrete Composites*, *59*, 18-25.

Collet, F., Chamoin, J., Pretot, S., & Lanos, C. (2013). Comparison of the hygric behaviour of three hemp concretes. *Energy and Buildings*, *62*, 294-303.

Crump, D., Dengel, A., & Swainson, M. (2009). Indoor air quality in highly energy efficient homes–a review. *United Kingdom: NHBC Foundation*.

DIN 18947: Earth Plasters - Terms And Definitions, Requirements, Test Methods. Berlin, Deutsches Institut für Normung

EN 1015 Methods of test for mortar for masonry. London: BSI

JIS A 1470-1 (2002). Test method of adsorption/desorption e ciency for building materials to regulate an indoor humidity-Part 1: Response method of humidity.

ISO 24353:2008. Hygrothermal performance of building materials and products — Determination of moisture ad- sorption/desorption properties in response to humidity variation. Internal standardization organization (ISO).

ISO 12572:2001. Hygrothermal performance of building materials and products — Determination of water vapour transmission properties. Internal standardization organization (ISO).

Karagiozis, A. and L. Gu. The EMPD model, in IEA/ECBCS Annex 41 Meeting. Glasgow, 2004.

Künzel, H. M., & Kießl, K. (1990). Bestimmung des Wasserdampfdiffusionswiderstandes von mineralischen Baustoffen aus Sorptionsversuchen. *Bauphysik*, *12*(5), 140-144.

Lanas, J., Perez Bernal, J. L., Bello, M. A., & Alvarez Galindo, J. I. (2004). Mechanical properties of natural hydraulic lime-based mortars. *Cement and concrete* research, 34(12), 2191-2201.

Latif, E., Lawrence, M., Shea, A., & Walker, P. (2015). Moisture buffer potential of experimental wall assemblies incorporating formulated hemp-lime. *Building and Environment*, *93*, 199-209.

Lourenço, P. B., Barros, J. O., & Oliveira, J. T. (2004). Shear testing of stack bonded masonry. Construction and Building Materials, 18(2), 125-132.

Maskell, D., Thomson, A., Lawrence, R., Shea, A. and Walker, P., 2015. The impact of bio-aggregate addition on the hygrothermal properties of lime plasters. In: 15th International Conference on Non-conventional Materials and Technologies (NOCMAT 2015), 2015-08-10 - 2015-08-13, University of Manitoba.

Maskell, D., Thomson, A. and Walker, P., 2017. Multi-criteria selection of building materials. Proceedings of the Institution of Civil Engineers: Construction Materials

McGregor, F., Heath, A., Shea, A., & Lawrence, M. (2014a). The moisture buffering capacity of unfired clay masonry. *Building and Environment*, *82*, 599-607.

McGregor, F., Heath, A., Fodde, E., & Shea, A. (2014b). Conditions affecting the moisture buffering measurement performed on compressed earth blocks. *Building and Environment*, *75*, 11-18.

McGregor, F., Heath, A., Maskell, D., Fabbri, A. and Morel, J.-C., 2016. A review on the buffering capacity of earth building materials. *Proceedings of the Institution of Civil Engineers: Construction Materials*, 169 (5), pp. 241-251.

Osanyintola, O. F., & Simonson, C. J. (2006). Moisture buffering capacity of hygroscopic building materials: Experimental facilities and energy impact. *Energy and Buildings*, *38*(10), 1270-1282.

Padfield, T. (1998). The role of absorbent building materials in moderating changes of relative humidity. *Department of Structural Engineering and Materials, Lyngby, Technical University of Denmark*, *150*.

Rode, Carsten, et al. *Moisture buffering of building materials*. Technical University of Denmark, Department of Civil Engineering, 2005.

Roels, S., & Janssen, H. (2006). A comparison of the Nordtest and Japanese test methods for the moisture buffering performance of building materials. *Journal of Building Physics*, *30*(2), 137-161.

Svennberg, K. (2006). *Moisture buffering in the indoor environment* (Vol. 1016). Byggnadsfysik LTH, Lunds Tekniska Högskola.

Thomson, A., Maskell, D., Walker, P., Lemke, M., Shea, A. and Lawrence, R., 2015. Improving hygrothermal properties of clay. In: 15th International Conference on Non-conventional Materials and Technologies (NOCMAT 2015), 2015-08-10 - 2015-08-13, Univeristy of Manitoba.

Wan, H., Xu, X., & Li, A. (2017). Application analysis of theoretical moisture penetration depths of conventional building material. Advances in Mechanical Engineering, 9(5), 1687814017699803.

Woloszyn, M., Kalamees, T., Abadie, M. O., Steeman, M., & Kalagasidis, A. S. (2009). The effect of combining a relative-humidity-sensitive ventilation system with the moisture-buffering capacity of materials on indoor climate and energy efficiency of buildings. *Building and Environment*, *44*(3), 515-524.

Woods, J., Winkler, J., & Christensen, D. (2013). Evaluation of the effective moisture penetration depth model for estimating moisture buffering in buildings. *Contract*, *303*, 275-3000.